

Power Supply and RF Signal Routing Architecture Design for Ultralight Deployable Ka-Band Active Phased-Array Transceivers

Hiroki Hayashi, Yasuto Narukiyo, Delburg Mitchao, Yuki Takeda, Sene Kato, So Yeon Suk, Hiraku Sakamoto,
Dongwon You, Kenichi Okada, and Atsushi Shirane
Tokyo Institute of Technology
Meguro, Tokyo, 152-8552, Japan
hayashi.h@ssc.pe.titech.ac.jp

ABSTRACT

The paper introduces a power supply and Radio Frequency (RF) signal routing architecture design for a foldable phased array transceiver intended for next-generation space communication systems. The transceiver is built using four 6-layer rigid-flexible substrates, enabling a high layer count and complex electrical routing. Using a DC-DC converter and changing the voltage from 5.5V to 1.2V reduces power loss by 43%. Three types of transmission lines are used to enable folding. These lines allow for complex, low-loss RF distribution. A prototype rigid flexible board was fabricated for evaluation, and power supply and RF were evaluated.

1. INTRODUCTION

Technological advancements have led to the miniaturization of electronic components and enabled the proliferation of small satellite constellations for space-based communications. However, high-performance antennas require large apertures and significant power to maintain high data rates and reliable connectivity in satellite communications. Deployable phased array antennas have emerged as a promising solution, as they can be stowed compactly during launch and then deployed in orbit, providing a larger effective aperture area without increasing the satellite's overall size.

One innovative design involves 4×2 phased arrays, which consist of two rigid boards connected by coaxial cables [1]. This approach aims to leverage the rigidity and stability of traditional antenna structures while incorporating the flexibility of deployable mechanisms. However, this design faces challenges such as the complexity of assembly and wiring and the need for low-loss power transmission to support the larger antenna's increased power demands. Despite its potential, this design faces challenges such as the complexity of assembly and wiring, as well as the need for low-loss power transmission.

Phased arrays using polyimide material for weight reduction have also been reported. By using lightweight polyimide, a significant weight per area reduction has been achieved. A 16 x 16 antenna array using polyimide material is presented in [2]. However, polyimide material has the problem of high loss in high-frequency signals and is not suitable for complex wiring due to the difficulty of multilayering. An 8 × 8 phased array TX combining 2- and 6-layer LCPs is proposed in [3]. 6

layers form a subarray, and 2 layers are foldable. The lightweight and large array size is achieved by forming subarrays in the 6-layer part and foldable in the 2-layer part. However, like [2], it is also difficult to integrate complex routing of RF and power lines due to the difficulty of multilayering. In addition, LCP is flexible but has the disadvantage of high RF loss.

Other phased arrays exist that use rigid-flexible substrates as the material for the phased array. For example, a technique to increase integration by using rigid sections only around components is discussed in [4]. This allows a lightweight and foldable structure with high integration. However, there is a problem of difficulty in wiring due to the small number of layers.

This study proposes a rigid-flexible substrate for power, RF, and thermal, evaluation for 64 x 64 active phased array TXs. This substrate includes three technologies. First, a six-layer rigid substrate is combined with a two-layer flexible substrate to enable foldable and complex routing. Next, assuming a large array antenna, the power required for the IC is transmitted at a low current value. DC-DC converters convert the current and voltage values to the specified values. The DC-DC converters reduce the power supply from 5.5V and 0.5A to 1.2V and 2A thereby minimizing power loss [5]. Finally, two substances are used to dissipate the heat of the IC. As described in detail in [6], carbon fiber and graphite sheets are used to smoothly transfer the heat generated by the IC to the heat dissipation surface.

The paper is organized as follows: Section 2 will provide details on the overall design of the TX and the layer composition of the rigid flexible substrate. Section 3 will introduce the power supply and RF routing. Section 4 will showcase the prototype created.

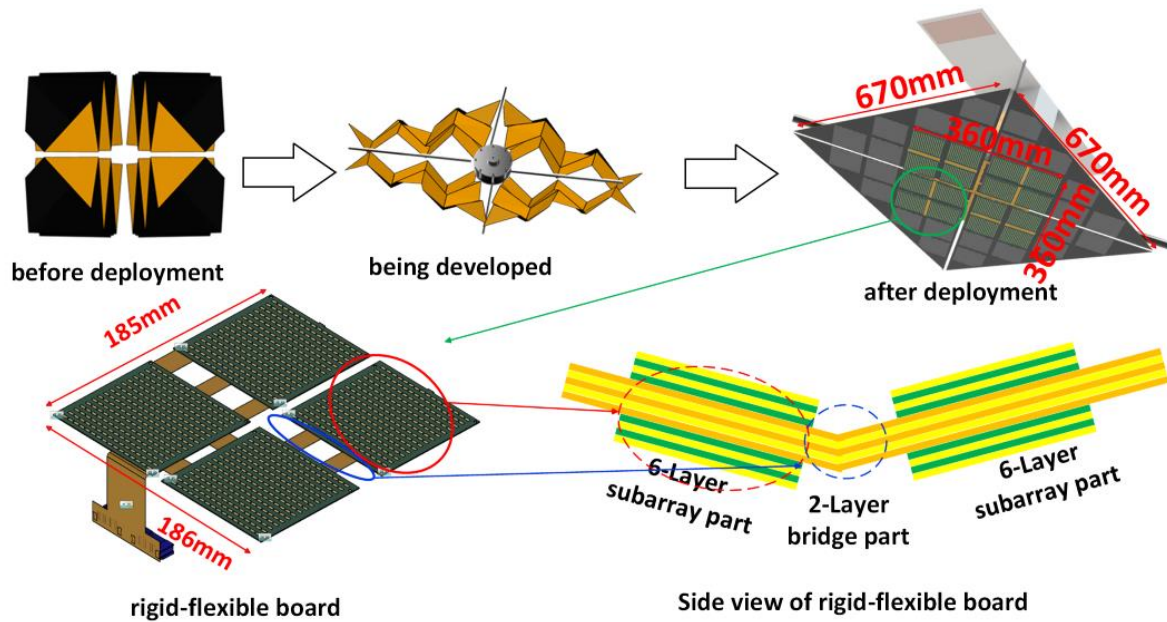


Figure 1: Design concept for a foldable phased array transceiver using a rigid-flexible substrate design, mounted on an origami-folded deployable antenna structure.

2 CONCEPTS

2.1 Mission Targets

Table 1: Targets of active phased-array transceivers

Parameter	Value
Size[mm]	Membrane: 670×670×2 Antenna: 360×360×0.64
Weigh[kg]	Membrane: < 2
Power[W]	< 450
Communication speed [Gbps]	4
Beam steering range [deg]	-70~ 70
Number of antenna elements	4096
EIRP [dBm]	> 80

Figure 1 presents a design concept of a rigid-flexible phased array antenna installed on a deployable structure inside a CubeSatellite. The deployable antenna structure is folded using the Miura fold [7] for compact storage before deployment in space. Once it reaches its designated low-earth orbit (LEO), it is deployed using four mechanical booms.

Table 1 provides an overview of the mission targets for the phased array antenna transceiver. The satellite adheres to the CubeSat standard and has a size of 6U (100mm x 200mm x 300mm). The deployable structure is initially stored in a 2U (100 mm x 200mm x 100mm)

volume. Once in low Earth orbit (LEO), the deployment curtain expands to a size of 670mm x 670mm. The antenna area within the deployable structure measures 36cm x 36cm in the center, with the remaining areas designated for heat dissipation. The total weight of the deployable antenna is designed to be less than 2 kg to ensure smooth deployment using the boom.

The communication speed target is 4 Gbps with a beam angle of -70° to 70° . The number of antenna elements is set at 64×64 , totaling 4096, and the target EIRP is 80 dBm. The transmitter (TX) is a phased array comprising 64×64 patch antennas divided into four 16×16 subarrays. Beamforming for the phased array is performed by the Beam-Forming IC (BFIC) [8], which is installed on the satellite body side of the rigid flexible substrate. A total of 512 BFICs drive all patch antennas. Figure 1 also depicts the deployment membrane, rigid-flexible substrate, subarray, and bridge sections. The subarray part contains components such as antenna patches and BFICs and has complex RF and Power routing. The bridge part is the fold of the Miura weave and provides simple electrical routing.

2.2 Layer Structure

Figure 2 shows a cross-sectional view of a 6-layer rigid flexible board. The board is made with a total thickness of 0.64mm. The layers, named L1, L2, L3, L4, L5, and L6, run from the IC side to the antenna side, using Megtron6 as the rigid material.

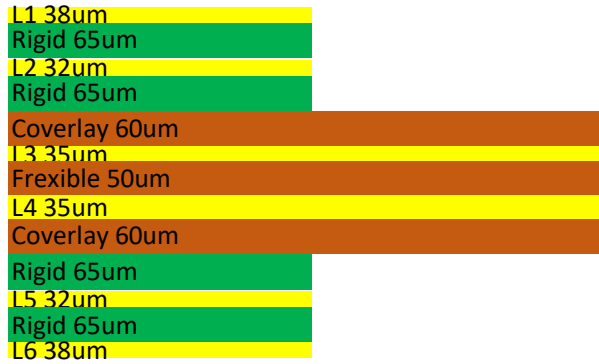


Figure 2: Side view of rigid-flexible board

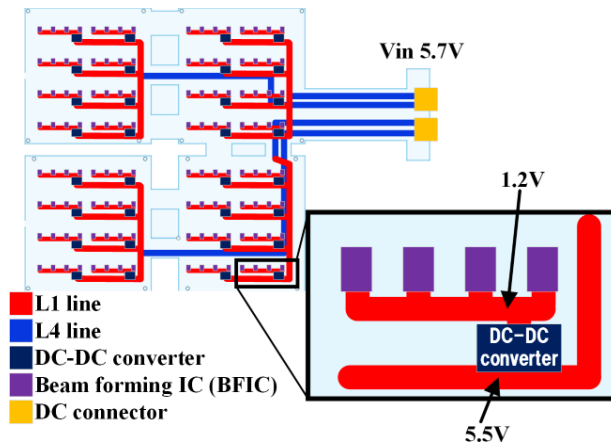


Figure 4: Power routing architecture

The only flexible material is between layers L3 and L4; all other layers use rigid material. Layers L1, L2, L5, and L6 are specifically used in the sub-array part, while L3 and L4 are dedicated to the bridge part. The subarray part contains components such as BFIC, DC-DC converters, and patch antennas, each with its dedicated electrical routing. On the other hand, the bridge part is responsible for facilitating power and signal routing between subarrays and has fewer layers, making it easier to fold.

3. TX DESIGN

3.1 Power

Figure 4 shows the power line routing, with L1 and L4 specifically designed for power to prevent conflicts with RF lines. The BFICs consume significant power, with each BFIC requiring 1.2V and 0.5A, totaling 307.2W for the entire transceiver. Thus, it is essential to prioritize routing to minimize power loss.

An increase in copper thickness can reduce loss, but it also leads to a larger bending radius, making it challenging to fold using Miura-folded. Additionally, the width of the power line is critical, and widening it can

Table 2: Simulation of power loss with and without DC-DC converter.

Parameter	without DC-DC converter	with DC-DC converter
Line loss [W]	642.78	43.37
DC-DC converter loss [W]	0	58.51
Total Loss [W]	642.78	101.88
BFIC Power [W]	307.20	307.20
Efficiency [%]	32	75

reduce loss, but mechanical limitations constrain this due to the board size. To mitigate power consumption, a DC-DC converter is used to transmit power at a lower current value. The DC-DC converter in this paper has a low height of 1.1 mm [5], meeting mechanical constraints. It can convert 5.5V and 0.5A to 1.2V and 2.0A, reducing the current value by 4 times. Since the current value is proportional to the power loss, the DC-DC converter can theoretically reduce the loss to one-sixteenth that of a system without a DC-DC converter.

Table 2 compares the power loss with and without the DC-DC converter. According to the datasheet of the DC-DC converter, the conversion efficiency of the DC-DC converter is calculated at 84%. [5]. Without the DC-DC converter, the power line consumes a significant 642.78W, whereas, with the DC-DC converter, it reduces to a mere 43.37W. Even considering the conversion efficiency, the loss reduction is significant, highlighting the effectiveness of the DC-DC converter in our project. Efficiency increases to 75% when a DC-DC converter is utilized, compared to 32% without it.

3.2 RF Routing

The diagram in Figure 3 shows the transmission line design. The RF signals output by the Field-Programmable gate array (FPGA), Digital-Analog converter (DAC), Analog-Digital (ADC), Mixer, and Amplifier on the satellite body are input through the RF connector on the rigid flexible board. Each subarray includes 256 patch antennas, which are powered by 32 BFICs. The RF Line consists of three lines: L1 microstrip line (L1_MSL), L3 strip line (L3_STL), and L3 microstrip line (L3_MSL). L2 corresponding to L1_STL, L2, and L4 corresponding to L3_STL, and L4 corresponding to L3_MSL are grounds. L1_MSL drives the antenna at the output of the BFIC, and RF distribution to the BFIC is done by L3_STL and L3_MSL. L3_MSL connects each subarray on bridge parts. Only L3 and L4 exist at the fold, with L4 serving as GND, both the L1_MSL to L3_STL

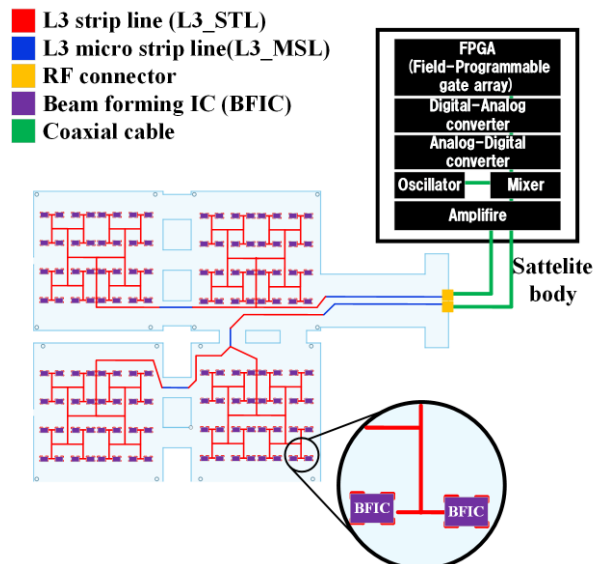


Figure 3: RF routing

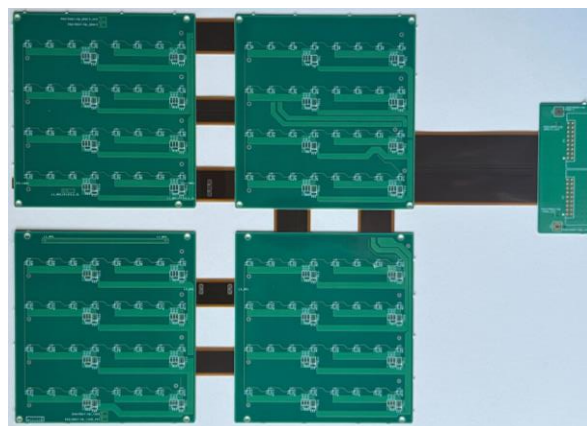
transition and the L3_MSL to L3_STL transition are impedance matched at 50Ω .

3.3 Thermal Conductivity

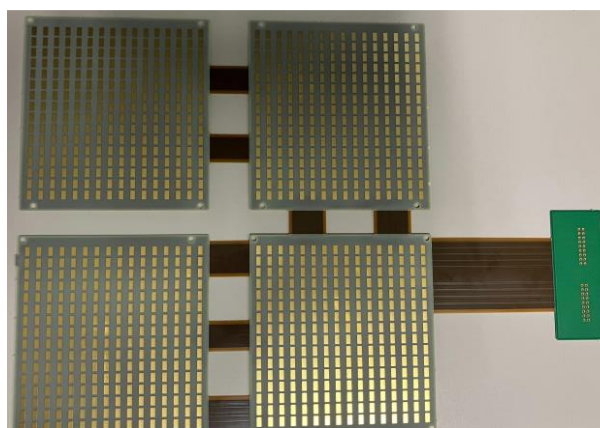
The operation of electrical components, such as BFICs, can be impacted by the heat they generate. Inadequate dissipation of this heat can result in less-than-optimal beamforming in phased arrays. To address this issue, a deployable composite structure is utilized, comprising graphite sheet laminates and graphite fiber [6]. Graphite sheets are known for their high thermal conductivity (10 times that of aluminum and 3 times that of copper). However, graphite sheets by themselves are brittle, so six layers are laminated to increase the thermal capacity and rigidity of the entire structure. In addition, carbon fiber is introduced to address the rigidity of the folded sections. Graphite sheets absorb sunlight quickly and therefore heat up when used in space. To cope with this, thin solar reflective films are attached to the upper and lower layers of the structure. These films have low absorption and high emissivity, which improves the thermal radiation of the structure and provides thermal control. This structure serves the dual function of a heat sink and a mounting structure.

4. RIGID-FLEXIBLE BOARD PROTOTYPE

The image in Figure 5 depicts a 64×64 Ka-band active phased array TX prototype that has been specially constructed to verify power distribution and RF loss within the design architecture. This board is used to evaluate thermal solutions to effectively dissipate the heat generated by the BFIC. For thermal testing and to assess RF and power loss, a MOS with identical power consumption to the BFIC is utilized. It is important to



(a) IC side



(b) Antenna side

Figure 5. Prototype of the rigid-flexible board

note that the antenna is inactive and non-functional and that the RF Line has been apertured with a metal pad at all critical points to minimize RF loss. This prototype board was used to measure power loss and RF signal loss and to perform thermal testing.

5. CONCLUSION

This study presented a design architecture for space-based phased array transceivers with low-loss and low-loss RF distribution. To allow for flexible folds, the study employs a combination of a 6-layer rigid substrate and a 2-layer flexible substrate. The DCDC converter achieves a power efficiency of 75%, compared to 32% without it. Three RF lines enable complex RF routing and facilitate large-scale phased arrays. To validate the design, a 64×64 Ka-band active phased array TX prototype using rigid flexible substrates was fabricated and evaluated for performance. This approach enables the large deployable phased arrays with Miura-folded while minimizing electrical losses. Reducing the cost of launching large, lightweight transceivers will allow more satellites to be launched at the same cost as before,

contributing to the dramatic development of the space industry.

Acknowledgment

This work is partially supported by NICT(JPJ012368C00601), MIC/SCOPE (192203002 and 192103003), JST A-STEP (JPMJTR211D), STAR, and VDEC in collaboration with Cadence Design Systems, Inc., Mentor Graphics, Inc., and Keysight Technologies Japan, Ltd.

References

[1] D. You, Y. Takahashi, S. Takeda, M. Moritani, H. Hagiwara, S. Koike, H. Lee, Y. Wang, Z. Li, J. Pang, A. Shirane, H. Sakamoto, and K. Okada, "A Ka-band 16-element deployable active phased array transmitter for satellite communication," in *IEEE MTT-S Int. Microw. Symp. Dig.*, Jun. 2021, pp. 799–802.

[2] A. Fikes, O. S. Mizrahi, and A. Hajimiri, "A framework for array shape reconstruction through mutual coupling," *IEEE Trans. Microw. Theory Techn.*, vol. 69, no. 10, pp. 4422–4436, Oct. 2021.

[3] D. You X. Fu, H. Herdian, X. Wang, Y. Narukiyo, A. Fadila, H. Lee, M. Ide, S. Kato, Z. Ki, Y. Wang, D. Awaji, J. Pang, H. Sakamoto, K. Okada, and A. Shirane, "A Ka-Band 64-Element Deployable Active Phased-Array TX on a Flexible Hetero Segmented Liquid Crystal Polymer for Small Satellites," in *IEEE Microwave and Wireless Technology Letters*, vol. 33, no. 6, pp. 903-906, June 2023,

[4] W. F. Moulder, R. N. Das, A. C. Maccabe, L. A. Bowen, E. M. Thompson, and P. J. Bell, "Rigid-Flexible Antenna Array (RFAA) for Lightweight Deployable Apertures," 2020 14th European Conference on Antennas and Propagation (EuCAP), 2020, pp. 1-5.

[5] Texas Instruments, "TPSM8282x, TPSM8282xA 1-A, 2-A, and 3-A High Efficiency Step-Down Converter MicroSiP™ Power Module with Integrated Inductor" Jun. 2024. Available: <https://www.ti.com/lit/ds/symlink/tpsm82822.pdf>

[6]Delburg P. Mitchao, Yuki Takeda, So Yeon Suk, Dongwon You, Atsushi Shirane, Hiraku Sakamoto, Yasushi Nishikawa, Masae Yano, and Saki Abe. "Highly Thermal Conductive Deployable Membrane for Large Ka-band Active Phased Array Antenna," AIAA 2024-0186. *AIAA SCITECH 2024 Forum*. January 2024.

[7] Mark S, Simon D. Guest, "Geometry of Miura-folded metamaterials," *Proceedings of the National*

Academy of Sciences, Vol. 110, No. 9, 2013, pp. 3276-3281 February 2013.

[8] X. Fu et al., "A 2.95mW/element Ka-band CMOS Phased-Array Receiver Utilizing On-Chip Distributed Radiation Sensors in Low-Earth-Orbit Small Satellite Constellation," 2023 IEEE International Solid-State Circuits Conference (ISSCC), San Francisco, CA, USA, 2023, pp. 18-20.